Title

Systemic delivery of proresolving lipid mediators resolvin D2 and maresin 1 attenuates intimal hyperplasia in mice

Journal

The FASEB Journal, 29(6)

ISSN

0892-6638

Authors

Akagi, Daisuke
Chen, Mian
Toy, Robert
et al.

Publication Date

2015-06-01

DOI

10.1096/fj.14-265363

Peer reviewed

The FASEB Journal article fj.14-265363. Published online March 16, 2015.

Systemic delivery of proresolving lipid mediators resolvin D2 and maresin 1 attenuates intimal hyperplasia in mice

Daisuke Akagi, Mian Chen, Robert Toy, Anuran Chatterjee, and Michael S. Conte[1]

Department of Surgery and Cardiovascular Research Institute, University of California, San Francisco, San Francisco, California, USA

ABSTRACT **Vascular injury induces a potent inflammatory response that influences vessel remodeling and patency, limiting long-term benefits of cardiovascular interventions such as angioplasty. Specialized proresolving lipid mediators (SPMs) derived from ω-3 polyunsaturated fatty acids [eicosapentaenoic acid and docosahexaenoic acid (DHA)] orchestrate resolution in diverse settings of acute inflammation. We hypothesized that systemic administration of DHA-derived SPMs [resolvin D2 (RvD2) and maresin 1 (MaR1)] would influence vessel remodeling in a mouse model of arterial neointima formation (carotid ligation). *In vitro*, SPM treatment inhibited mouse aortic smooth muscle cell migration ($IC_{50} \cong 1$ nM) to a PDGF gradient and reduced TNF-α–stimulated p65 translocation, superoxide production, and proinflammatory gene expression (MCP-1). *In vivo*, adult FVB mice underwent unilateral carotid artery ligation with administration of RvD2, MaR1, or vehicle (100 ng by intraperitoneal injection at 0, 1, 3, 5, and 7 days after ligation). In ligated carotid arteries at 4 days, SPM treatment was associated with reduced cell proliferation and neutrophil and macrophage recruitment and increased polarization of M2 macrophages in the arterial wall. Neointimal hyperplasia (at 14 d) was notably attenuated in RvD2 (62%)- and MaR1 (67%)-treated mice, respectively. Modulation of resolution pathways may offer new opportunities to regulate the vascular injury response and promote vascular homeostasis.—Akagi, D., Chen, M., Toy, R., Chatterjee, A., Conte, M. S. Systemic delivery of proresolving lipid mediators resolvin D2 and maresin 1 attenuates intimal hyperplasia in mice. *FASEB J.* 29, 000–000 (2015). www.fasebj.org**

Key Words: neointimal hyperplasia · inflammation · vascular remodeling · fatty acid

Peripheral arterial disease (PAD) is increasing in prevalence on a global scale because of a combination of population aging, diabetes, and lifestyle-related risk factors (1). Modalities of treatment for patients with symptomatic PAD include exercise, medical, surgical, and endovascular interventions (2). Although the utilization of invasive PAD treatments is steadily rising, limited durability of both endovascular and bypass surgery procedures remains a common and increasingly costly problem (3). It is established that atherosclerosis is an inflammatory disease (4). The pathologic hallmark of these vascular treatment failures is neointimal hyperplasia, an excessive healing response that has been linked to inflammation. The attenuation of neointimal hyperplasia after various clinical forms of vascular injury remains a critical scientific need in the management of advanced PAD, as well as other chronic forms of atherosclerosis (*e.g.,* coronary, cerebral).

Recent evidence suggests that the resolution of inflammation is an active process, partly organized by specialized proresolving lipid mediators (SPMs) derived from n-6 and n-3 polyunsaturated fatty acids (PUFAs) (5). SPMs include 4 distinct biochemical families: lipoxins, protectins, resolvins, and maresins (5–7). Resolvins were identified from resolving exudates in self-limited murine inflammation models and divided into 2 groups by synthetic pathway: D-series resolvins (RvD) are derived from docosahexaenoic acid (DHA) and E-series resolvins (RvEs) from eicosapentanoic acid (EPA) (5, 6). Various reports have shown beneficial effects *of* RvDs and RvEs *in vivo* across a broad range of animal models of inflammation (6). Maresins (*e.g.,* MaR1) are a recently identified genus of SPM, also delivered from DHA *via* a novel epoxide intermediate (7). MaR1 has shown homeostatic activity in models such as acute lung injury, colitis, and tissue regeneration (8–10). Vascular effects of MaR1 have not been reported previously.

Local biosynthesis of lipid mediators, including lipoxin A4, RvD1, and protectin D1 protects against atherosclerosis in apolipoprotein E-deficient mice (11). In earlier work, we demonstrated that vascular smooth muscle cell (VSMC) phenotype may be directly modulated by SPMs (lipoxins and resolvins) and that levels of 1 SPM (lipoxin A4) were

Abbreviations: AA, arachidonic acid; Arg-1, arginase-1; ASMC, aortic smooth muscle cell; DHA, docosahexaenoic acid; DHE, dihydroethidium; EPA, eicosapentanoic acid; FBS, fetal bovine serum; MaR1, maresin 1; MCP-1, monocyte chemotactic protein-1; PAD, peripheral arterial disease; PDGF, platelet-derived growth factor; PTX, pertussis toxin; PUFA, polyunsaturated fatty acid; Rv, resolvin; SMC, smooth muscle cell; SPM, specialized lipid mediators; VSMC, vascular smooth muscle cell

[1] Correspondence: Department of Surgery and Cardiovascular Research Institute, University of California, San Francisco, 400 Parnassus Ave., Suite A-581, San Francisco, CA 94143. E-mail: michael.conte2@ucsf.edu

doi: 10.1096/fj.14-265363

This article includes supplemental data. Please visit *http://www.fasebj.org* to obtain this information.

inversely correlated with the severity of peripheral atherosclerosis in patients (12). More recently, we reported that the D-series resolvins RvD1 and RvD2 exhibited a broad range of effects on VSMC (anti-inflammatory, antimigratory, and antiproliferative) and attenuated neointimal hyperplasia in a rabbit balloon injury model, when delivered directly to the injured artery (13). Here we sought to examine the hypothesis that resolution of a local vascular injury could be enhanced by systemic administration of SPM (RvD2 and MaR1), using a mouse model of flow-induced remodeling. This report supports the translational concept of augmenting biochemical pathways of resolution in the setting of vascular injury.

MATERIALS AND METHODS

Mouse aortic smooth muscle cell isolation and culture

Mouse aortic smooth muscle cells (ASMCs) were isolated from aorta of adult male FVB mice as described previously (14). Aortas were harvested and dispersed by enzymes with collagenase, soybean trypsin, and elastase in DMEM containing 20% fetal bovine serum (FBS). The adventitial layer was stripped off after incubation with enzymes for 10 minutes, and then the endothelial layer was scraped. Tissues were incubated in enzymatic solution again for 1 h, and ASMCs were collected. Primary mouse ASMCs were maintained in DMEM (low glucose; HyClone Laboratories, Logan, UT, USA) containing 10% FBS (Invitrogen Life Technologies, Grand Island, NY, USA) and used between passages 3 and 6.

Chemicals

RvD2 (7*S*,16*R*,17*S*-trihydroxy-4*Z*,8*E*,10*Z*,12*E*,14*E*,19*Z*-DHA) and MaR1 (7*R*,14*S*-dihydroxy-4*Z*,8*E*,10*E*,12*Z*,16*Z*,19*Z*-DHA) were purchased from Cayman Chemical Company (Ann Arbor, MI, USA).

Migration assays

ASMC migration was evaluated using a modified Boyden assay with 8 μm pore transwell inserts, as described previously (15). Cells were pretreated with RvD2 or MaR1 (0.01, 1, or 100 nM) for 30 min before the addition of platelet-derived growth factor-BB (PDGF-BB, 50 ng/ml; Sigma-Aldrich, St. Louis, MO, USA) as a chemoattractant to the bottom wells. All test compounds were present in both top and bottom wells for the full duration of chemotaxis experiments (6 h). In some experiments, pertussis toxin (PTX, 100 ng/ml; Calbiochem EMD Chemicals, San Diego, CA, USA) was added to the cells 30 min before the addition of RvD2 and MaR1. All treatment conditions were performed in triplicate.

The scratch (wound) assay was used as a complementary approach to evaluate ASMC migration, as described previously (16). Cells were plated at confluent status for 24 hours and then pretreated with RvD2 or MaR1 (100 nM) for 30 minutes before the addition of PDGF-BB (50 ng/ml; Sigma-Aldrich) as a chemoattractant, simultaneous with creation of a 900 μm wound in the plate using a 200 μl pipette tip. Cell migration area was evaluated 24 hours after scratching was performed. All treatment conditions were performed in quadruplicate.

Superoxide production

ASMCs were seeded and grown on chamber slides at a density of 10,000 cells per chamber for 2 days, followed by treatment with 10 ng/ml TNF-α with or without RvD2 and MaR1 (10–500 nM) in serum-free medium for 18 hours. ASMCs were incubated with dihydroethidium (DHE; 5 μM; Invitrogen) in serum-free medium for 30 minutes at 37°C in a humidified chamber protected from light. DAPI nuclear counterstaining was used. Fluorescence was detected with a tetramethylrhodamine isothiocyanate filter allowing the detection of the DHE emission wavelength of 590–620 nm. The fluorescence lamp gain was standardized for all images and analyses. Fluorescence intensity was quantified using ImageJ software (National Institutes of Health, Bethesda, MD, USA). For ASMCs, the fluorescence intensity was determined for untreated DHE-stained cells from each experimental group, and intensity measurements from treated cells were then normalized to the corresponding value.

Nuclear translocation of p65

Activation of the transcription factor NF-κB involves translocation of the p65 subunit from cytoplasm to nucleus, which may be detected by immunofluorescent staining of p65 (17). ASMCs were seeded and grown on chamber slides at a density of 10,000 cells per chamber for 2 days, followed by treatment with 10 ng/ml TNF-α with or without RvD2 and MaR1 (10–500 nM) for 4 hours. After incubation, cells were fixed with ice-cold acetone and incubated with p65 antibody (1:50; Santa Cruz Biotechnology, Dallas, TX, USA) overnight. For immunofluorescent staining, cells were incubated with Alexa Fluor 488 anti-goat IgG at 1:200 (Invitrogen) for 1 hour. The intensity of FITC fluorescence was measured by ImageJ software, and the ratio of fluorescence intensity of nucleus to cytoplasm was calculated. More than 200 cells were analyzed in 4 high-power pictures for each group.

Analysis of proinflammatory gene expression by quantitative RT-PCR

ASMCs were plated onto 6-well plates at semiconfluency in DMEM plus 10% FBS. Cells were then made quiescent by placing them in serum-free medium for overnight before the start of the experiments. Cells were pretreated with or without RvD2 or MaR1 at 10 or 100 nM for 30 minutes, followed by the addition of cytokine (TNF-α, 5 ng/ml) for 18 h. Total RNA was isolated with the RNeasy Mini Kit (Qiagen, Germantown, MD, USA) with RNase-free DNase treatment according to the manufacturer's protocol. Total RNA was used to generate cDNA using the High Capacity cDNA Reverse Transcription Kit (Applied Biosystems, Foster City, CA, USA) for subsequent quantitative RT-PCR. Amplified DNA was detected by incorporation of SYBR Green (Qiagen). Dissociation curve analyses were performed to confirm the specificity of the SYBR Green signal. Data were normalized to 2 reference genes (hypoxanthine phosphoribosyltransferase 1 and acidic ribosomal protein). The primers used are listed in Table 1. All of the primer pairs spanned across introns.

Animal experiments

All animal experiments were performed under a protocol approved by the University of California–San Francisco Animal Care Committee. FVB male mice (Charles River Incorporated, Hollister, CA, USA), 6–8 weeks of age, and maintained on a normal diet (5053, LabDiet, St. Louis, MO, USA) were used in all experiments. Animals were anesthetized for surgical procedures with inhalation of isoflurene for appropriate anesthetic depth. The carotid ligation model was performed as described previously (18). A midline incision of the neck was made, and the left common carotid artery was exposed and ligated just proximal to

TABLE 1. *Primers used in quantitative RT-PCR*

Primer	Forward sequence	Reverse sequence
ICAM-1	CTGCCTTGGTAGAGGTGACTGA	AGGACAGGAGCTGAAAAGTTGTAGA
IL-6	CCTCTCTGCAAGAGACTTCCAT	GTCTCCTCTCCGGACTTGTG
MCP-1	TCCCAAAGAAGCTGTAGTTTTTGTC	GGGCAGATGCAGTTTTAAATAAAGT
VCAM-1	TTCACGTGGGGCACAAAGAA	AGCTTGAGAGACTGCAAACAG
Hypoxanthine phosphoribosyltransferase 1	GGGATTTGAATCACGTTTGTGT	AACAGGACTCCTCGTATTTGC
Acidic ribosomal protein	AGACCTCCTTCTTCCAGGCTTT	CCCACCTTGTCTCCAGTCTTTATC

the bifurcation of internal and external carotid arteries with 7-0 polypropylene suture. In some groups of experiments, the bifurcations of left carotid arteries of mice were only exposed but not ligated (sham operation).

Systemic administration of SPMs

RvD2 or MaR1 (100 ng/mouse for each dose) was administered by the intraperitoneal route. As controls, vehicle (normal saline with 0.1% ethanol) was also administered. These SPMs or vehicle solutions were administered 4 hours prior to the carotid ligation (day 0) and then at 1, 3, 5, and 7 days after operation.

For evaluation of acute effects, mice ($n = 4$/group) were killed at 4 day after injury by inhalation of carbon dioxide. Injured carotid arteries were harvested, and cryosections were prepared for immunohistochemistry. For evaluation of neointimal hyperplasia and vessel remodeling, mice were killed at 14 days after injury ($n = 10$/group), and the tissue was perfusion fixed in 10% formalin. Vessels were then fixed overnight in 10% formalin and processed for embedding and sectioning.

Immunohistochemical staining

Immunofluorescent staining on specimens harvested at 4 days was performed on 6 μm thick frozen sections fixed by ice-cold acetone. Anti-neutrophil antibody (NIMP-R14, 1:100; Abcam, Boston, MA, USA) was used for detection of neutrophil infiltration. MOMA-2 (1:100; Cedarlane, ON, Canada) and anti-liver arginase antibody (Arg-1, 1:300; Abcam) were used for detection of macrophage/monocyte and M2 macrophage, respectively. Anti-Ki67 (1:80; Abcam) was used for detection of proliferating cells. After using proper biotinylated secondary antibodies, goat anti-mouse IgG-conjugated streptavidin-conjugated Alexa Fluor 594 (1:100; Invitrogen) and fluorescent streptavidin (1:100; Vector Laboratories, Burlingame, CA, USA) was used. DAPI (Invitrogen) nuclear counterstaining was used on all the immunofluorescent staining. Photography was performed with Olympus BX51 microscope (Olympus America, Center Valley, PA, USA) with an EXFO X-cite 120 system (EXFO Photonic Solutions, Mississauga, ON, Canada), Olympus DP70 digital microscope camera, and DPController software (Olympus). Three sections taken 1000 μm proximal to the ligature were used for analysis. To determine the precise location of sections, the number of sliced sections was counted using the microtome, measuring the distance. The macrophage/monocyte and neutrophil infiltration index was calculated as the ratio of the number of positively stained cells to the total number of DAPI-positive nuclei. The proportion of Ki67-positive cells was also calculated with DAPI-positive cell number.

Perfusion-fixed specimens harvested at 14 d were processed for immunohistochemistry to identify proliferating cells and smooth muscle identity in the neointimal lesions. The primary antibody used for VSMC identification was monoclonal anti-actin, α-smooth muscle-Cy3 antibody produced in the mouse (Sigma-Aldrich). The M.O.M. immunodetection kit (Vector Laboratories) was used, and final staining was done with 3-amino-9-ethylcarbazole, counterstained with hematoxylin. To identify the relationship of proliferating cells and VSMCs, double staining with anti-Ki67 antibody (1:10) and anti-actin, α-smooth muscle-Cy3 antibody (1:750) was also performed. After using proper biotinylated secondary antibodies, streptavidin-conjugated AlexaFluor 594 for α-smooth muscle cell actin and fluorescent streptavidin for Ki67 were used, with DAPI nuclear counterstaining.

Morphometry

Morphology was evaluated from 6 μm thick cross-sections of injured arteries harvested at 14 d, centered at 2500 μm from the ligature. Elastin staining was performed on cross sections of perfusion-fixed common carotid arteries with the elastic stain kit (Thermo Fisher Scientific, Runcorn, Cheshire, United Kingdom). Areas of neointima, media, adventitia, and lumen of carotid arteries were measured by ImageJ software. Each value was calculated as the average of 3 sections measured per vessel.

Statistical analysis

Data are shown as means ± SE. Direct comparisons were made using an unpaired Student t test. Multiple comparisons were made with the Dunnett *post hoc* test. In all cases, $P < 0.05$ was considered significant.

RESULTS

RvD2 and MaR1 attenuate mouse ASMC migration

Chemotaxis of ASMC toward a PDGF-BB gradient was significantly reduced by RvD2 and MaR1 pretreatment in a dose-dependent manner. The maximum percentage reduction in the cell migration assay was 74% for 100 nM RvD2 ($P < 0.01$) and 80% for 100 nM MaR1 ($P < 0.01$). The IC_{50} observed for this effect was 1 nM. The effects of RvD2 or MaR1 on PDGF-BB–induced chemotaxis were sensitive to inhibition by PTX, demonstrating a role for G-protein coupled receptors in modulating this response (**Fig. 1*A*, *B***).

In a similar fashion, both SPMs reduced wound closure of mouse ASMCs in the scratch assay. The area covered with migrated cells was reduced by 100 nM RvD2 (36% reduction, $P < 0.01$) and MaR1 (28% reduction, $P < 0.05$) treatment, respectively (Fig. 1*C*).

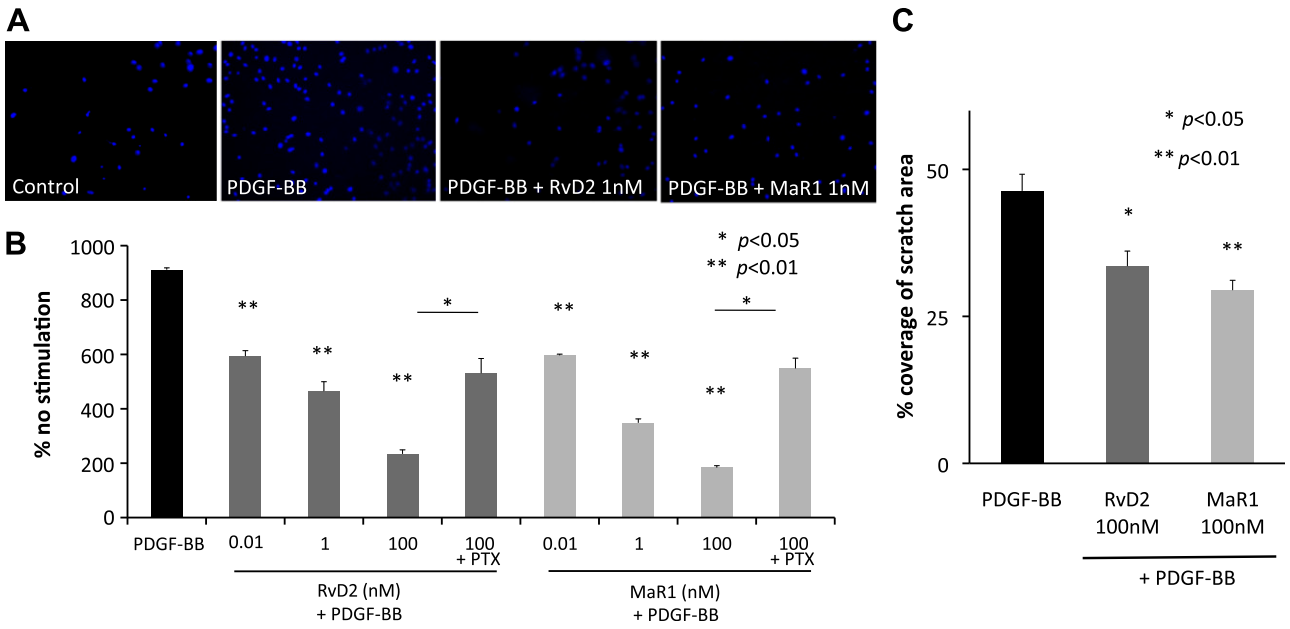

Figure 1. RvD2 and MaR1 reduce chemotaxis of mouse ASMC to PDGF-BB *in vitro*. *A*) ASMC migration response to PDGF-BB (50 ng/ml, 4 hours) with RvD2 (1 nM) or MaR1 (1 nM) pretreatment, using a transwell assay with Boyden chambers. Representative images stained with DAPI. *B*) Results of the transwell assay are expressed as percentage change in migration from unstimulated control (no PDGF). Inhibition of chemotaxis is shown for both RvD2 and MaR1 in dose-dependent manner ($n = 3$). Inhibition is PTX sensitive. *C*) In the ASMC scratch assay, wound closure was significantly reduced by RvD2 and MaR1 treatments. (*$P < 0.05$, **$P < 0.01$ *vs.* control; Dunnett *post hoc* test. Unpaired *t* test between RvD2 or Mar1 100 nM with PTX *vs.* without PTX in *B*.

RvD2 and Mar1 have modest antiproliferative effects on mouse ASMC *in vitro*

Serum (10%) stimulated proliferation of cultured ASMCs was reduced by exposure to both RvD2 (10% inhibition RvD2 at 500 nM; $P < 0.05$) and MaR1 (12% inhibition in MaR1 at 100 nM; $P < 0.05$; Supplemental Fig. S1).

Anti-inflammatory effects of RvD2 and MaR1 in cultured mouse ASMCs

Inflammatory cytokines such as TNF-α activate molecular pathways in ASMCs that potentiate the local response, including the induction of chemokines, cytokines, adhesion molecules, and oxidant stress. Reactive oxygen species such as superoxide enhance inflammation *via* secondary amplification pathways in the vessel wall. RvD2 or MaR1 pretreatment of ASMCs significantly reduced TNF-α–induced superoxide production across the range (10–500 nM) of tested SPM doses (% reduction: RvD2 46% at 500 nM and MaR1 53% at 500 nM; **Fig. 2 *A, B***).

We examined the activity of the key transcription factor NF-κB, which is known to regulate inflammatory pathways in ASMCs (Fig. 2*C, D*). Treatment with RvD2 or MaR1 significantly blunted TNF-α–stimulated p65 nuclear translocation compared with controls, in a dose-dependent fashion (% inhibition: RvD2 24% at 500 nM and MaR1 28% at 500 nM). We also examined TNF-α–stimulated expression of selected target genes in ASMCs, including intercellular adhesion molecules and proinflammatory cytokines, using quantitative real-time RT-PCR (Fig. 2*E*). Induced expression of the key chemokine monocyte chemotactic protein-1 (MCP-1) was significantly attenuated by both RvD2 and MaR1 (% attenuation: 44% for RvD2 at 100 nM, 39% for MaR1 at 100 nM). No significant differences were seen for IL-6, vascular VCAM-1, and ICAM-1 expression following TNF-α stimulation.

SPM treatment alters leukocyte recruitment to injured carotid arteries

The mouse carotid ligation model was used to examine the influence of systemic SPMs on local inflammation and remodeling. Systemic administration of both RvD2 and MaR1 significantly reduced acute leukocyte recruitment in the ligated carotid arteries at 4 d. Neutrophil infiltration (NIMP-R14) was reduced 48% by RvD2 and 56% by MaR1 (**Fig. 3*A***, *C*). Monocyte/macrophage infiltration (MOMA-2) was also reduced 48% by RvD2 and 43% by MaR1 (Fig. 3*B, D*). Active SPM treatment appeared to influence the polarization (M1 *vs.* M2) of macrophages within the injured artery wall. Although the absolute number of M2 macrophages (Arg-1) was reduced 49% by RvD2 and 51% by MaR1 (Fig. 3*D*), the proportion of M2 macrophages to total MOMA(+) cells was increased in arteries from RvD2= (64%) or MaR1- (51%) treated mice compared with vehicle-treated controls (43%; Fig. 3*E*).

SPM treatment reduces the proliferative response to arterial injury *in vivo*

Proliferating cells in injured arterial walls were detected by immunostaining of Ki67 (**Fig. 4*A, B***). Systemic RvD2 and MaR1 treatment reduced the early proliferative

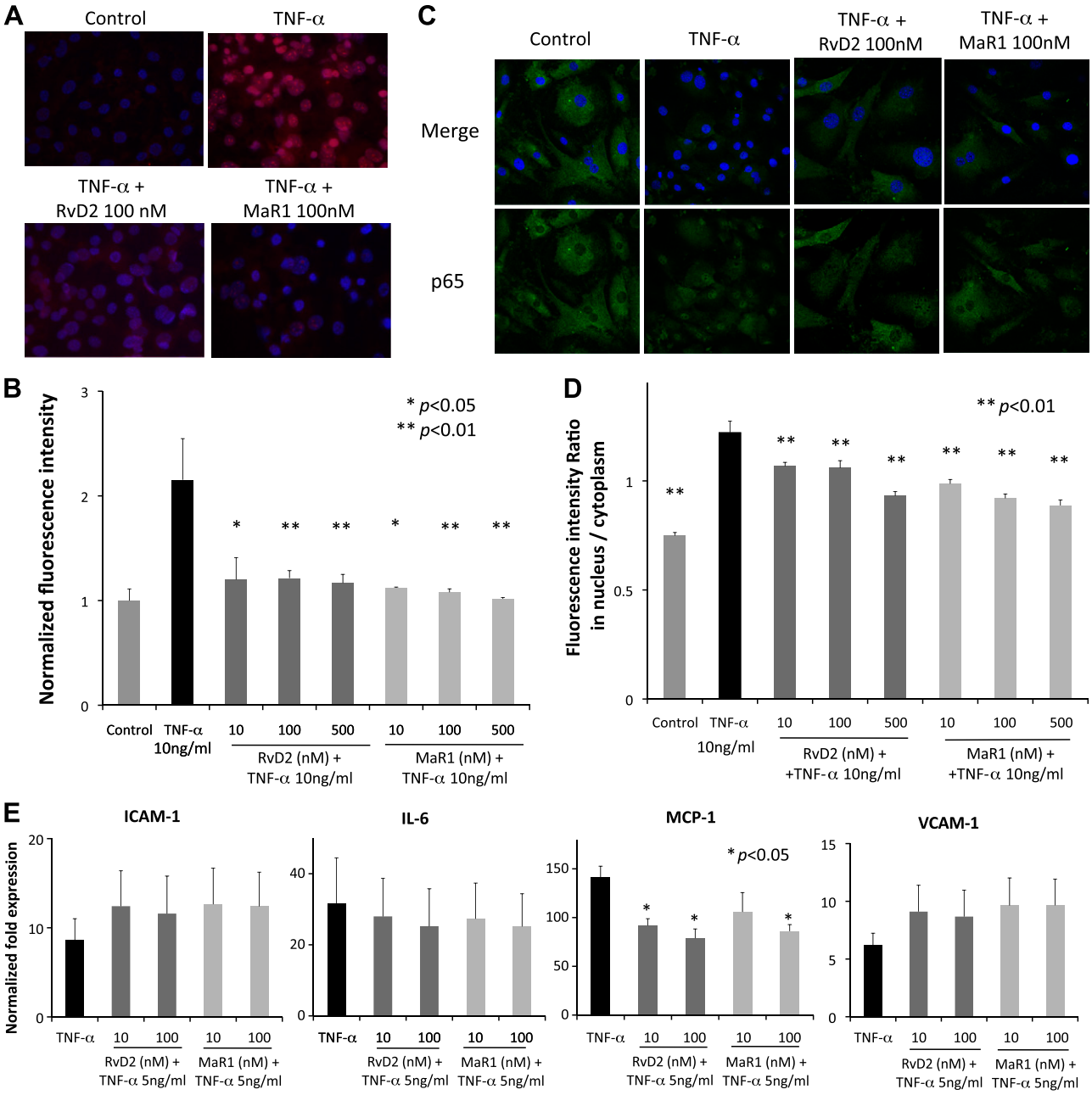

Figure 2. Cytokine activation of mouse ASMCs is altered by RvD2 and MaR1 *in vitro*. *A, B*) RvD2 or MaR1 treatment reduces TNF-α–induced superoxide production in cultured ASMCs. Superoxide production was evaluated by DHE staining. ASMCs were stimulated with TNF-α (10 ng/ml, 18 h) in the presence or absence of RvD2 or MaR1. *A*) Representative merged images of DHE staining, counterstained with DAPI. Negative control (no treatment), positive control (TNF-α only), TNF-α with RvD2 (100 nM), and TNF-α with MaR1 (100 nM). *B*) Quantitative comparison of DHE staining intensity normalized to control. $^*P < 0.05$, $^{**}P < 0.01$ *vs.* positive control (TNF-α); Dunnett *post hoc* test. Results shown are means ± SE. *C, D*) RvD2 and MaR1 modulate p65 translocation in ASMCs. Representative merged images of p65 translocation assay, counterstained with DAPI. *C*) Positive control (TNF-α 10 ng/ml for 4 hours), negative control (no treatment), TNF-α with 100 nM RvD2, and TNF-α with 100 nM MaR1. *D*) Quantitative comparison represented by the ratio of p65 fluorescence intensity of nucleus to cytoplasm. $^*P < 0.05$, $^{**}P < 0.01$ *vs.* control; Dunnett *post hoc* test. Results are means ± SE. *E*) Proinflammatory gene expression in ASMCs was modulated by RvD2 and MaR1. ASMCs were stimulated with TNF-α (5 ng/ml) for 18 hours in the presence or absence of RvD2 or MaR1 (100 or 10 nM, respectively), and quantitative PCR was performed. Proinflammatory gene expression of IL-6, ICAM-1, MCP-1, and VCAM-1 were measured. Shown is a significant attenuation in the expression of MCP-1 at 10 and 100 nM RvD2 and at 100 nM MaR1, with a nonsignificant trend of decrease in IL-6, ICAM-1, and VCAM-1 ($n = 5$). $^*P < 0.05$ *vs.* control; Dunnett *post hoc* test. Results are means ± SE.

response in ligated carotid arteries at 4 days. The ratio of Ki67-positive cells to total cells was decreased 77% by RvD2 and 52% by MaR1 compared with the vehicle-treated group. To investigate the identity of proliferating cells in the neointima and media, we performed double staining for Ki67 and α-SMC actin. Proliferating cells in the ligated arteries at 14 days were identified as mostly VSMCs (Supplemental Fig. S2).

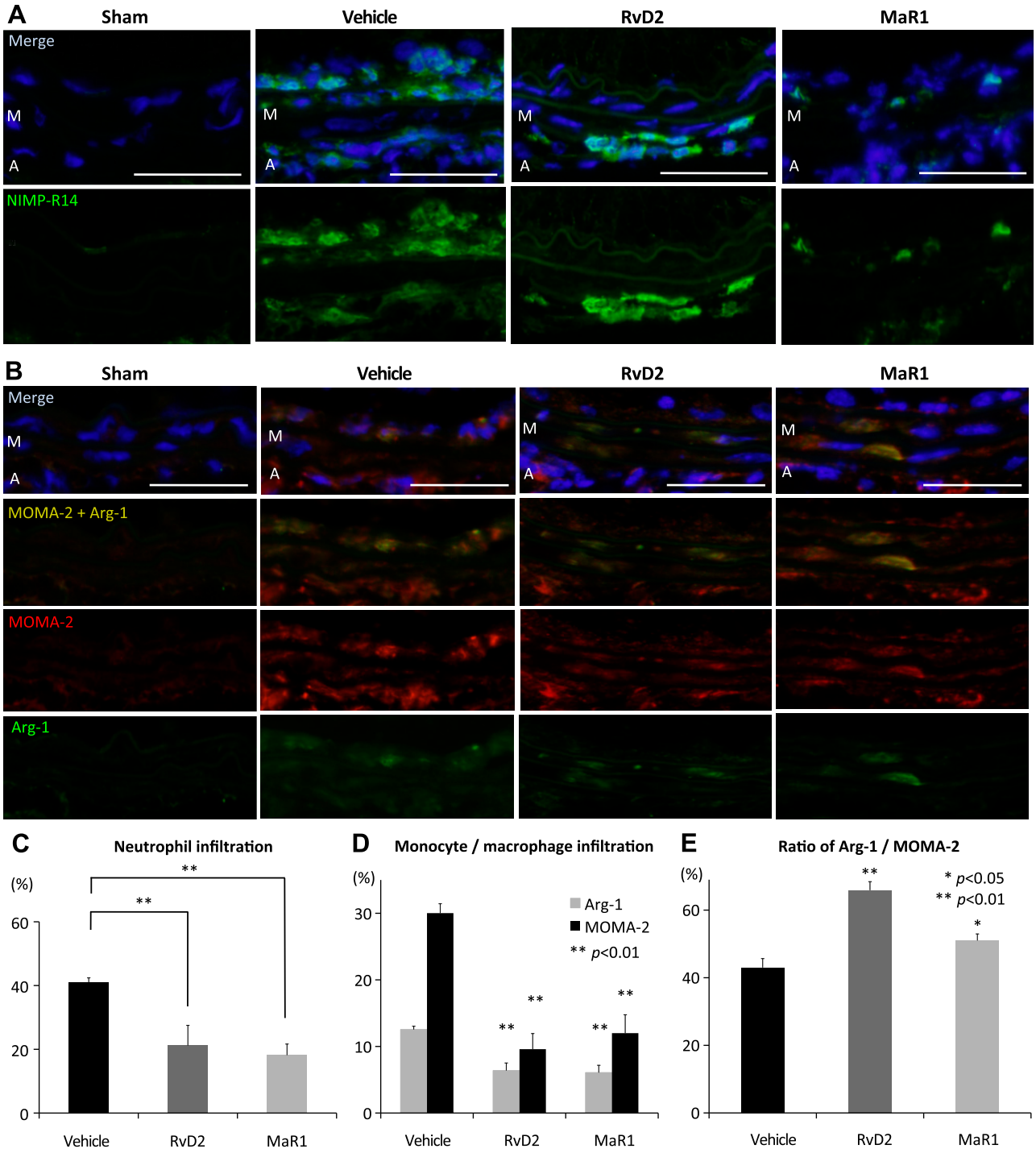

Figure 3. Systemic RvD2 and MaR1 treatment altered acute leukocyte recruitment and macrophage phenotype following carotid ligation in mice. *A*) Neutrophils were detected by immunostaining of NIMP-R14. Pictures of nonligated arteries (sham operation) were shown as negative controls. Ligated carotid arteries treated with vehicle served as positive controls. All samples were counterstained with DAPI (bar, 40 μm). *B*) Total monocytes/macrophages were detected by MOMA-2 and M2 macrophages were also detected by liver Arg-1 (bar, 40 μm). *C*) Quantification of neutrophil infiltration was shown as ratios of NIMP-R14–positive cells to total cells (DAPI) numbers. The extent of neutrophil infiltration was reduced by either RvD2 (48% reduction) or MaR1 (56% reduction) treatments. *D*) Quantification of total monocyte/macrophage infiltration or M2 macrophage was shown as ratios of positive cells of MOMA-2 or Arg-1 to total cells (DAPI) numbers. The ratio of MOMA-2 positive cells was reduced by RvD2 (48% reduction) or MaR1 (43% reduction) treatments. This overall reduction in monocyte/macrophage number included the Arg-1–positive subset. *E*) The ratio of M2 macrophages was calculated as the ratio of Arg-1–positive to MOMA-2–positive cells. The relative proportion of M2 in ligated carotid arteries was higher in RvD2- (53% higher) or MaR1- (19% higher) treated animals than in controls. Values were measured as average of 3 sections for 1 artery ($n = 4$). $^*P < 0.05$, $^{**}P < 0.01$ *vs.* control; Dunnett *post hoc* test. Results are means ± SE. M, media; A, adventitia.

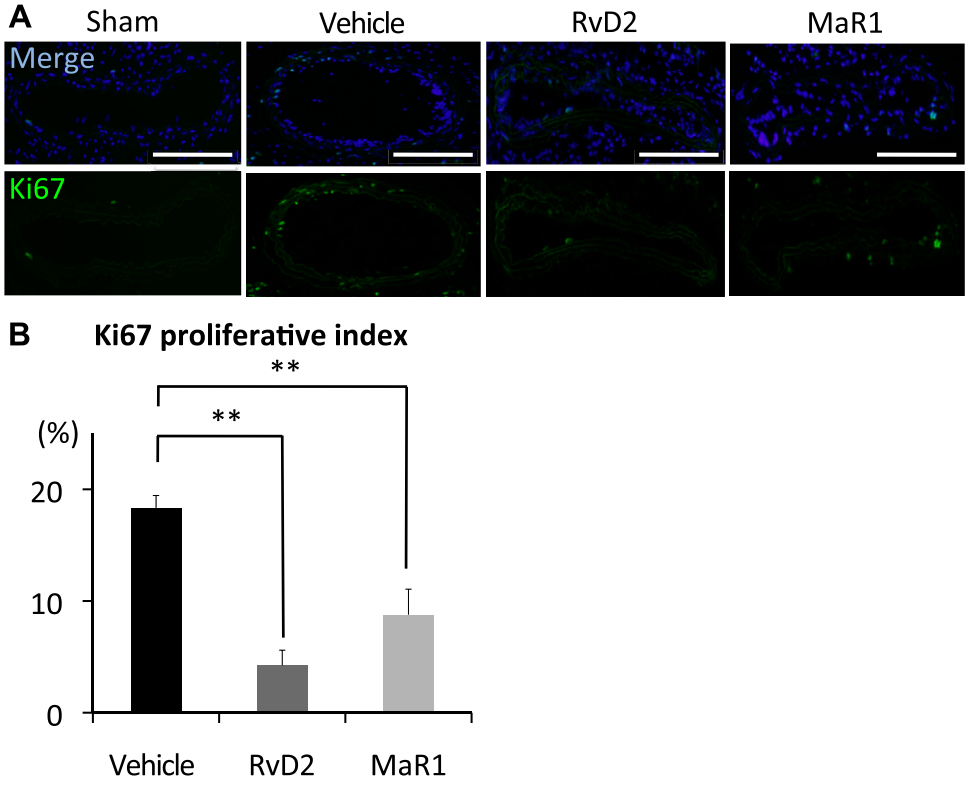

Figure 4. Systemic RvD2 and MaR1 treatment reduces the early proliferative response in ligated carotid arteries at 4 days. *A*) Proliferating cells are shown by immunostaining of Ki67. All samples were counterstained with DAPI. Images of nonligated arteries (sham operation) are shown as negative controls. Vehicle treatment is shown as positive control (bar, 100 μm). *B*) Quantification of Ki67-positive cells to total cells (DAPI) numbers. The Ki67 proliferation indices were reduced by RvD2 (77% reduction) or MaR1 (52% reduction) treatments. Values were measured as an average of 3 sections for each artery ($n = 4$). $^*P < 0.05$, $^{**}P < 0.01$ *vs.* control; Dunnett *post hoc* test. Results are means ± SE.

Vessel remodeling in ligated carotid arteries was modulated by systemic RvD2 and MaR1 treatment

Representative images of perfusion-fixed ligated carotid arteries, stained for elastin and SMC-actin, are shown (**Fig. 5*A, B***). Neointimal hyperplasia occurred in the ligated arteries at 14 days and was comprised primarily of actin(+) VSMCs. Robust neointimal hyperplasia developed in control mice, which was notably reduced in both active SPM treatment groups.

Morphometric analysis demonstrated that systemically administered RvD2 or MaR1 significantly attenuated neointimal hyperplasia at 14 days after carotid artery ligation (Figs. 5*A* and **6*A, B***). The neointima/media area ratio was significantly reduced in RvD2- and MaR1-treated mice (67% by RvD2 and 71% by MaR1). Carotid artery neointimal area was specifically reduced (0.028 mm^2 by RvD2 and 0.024 mm^2 by MaR1 *versus* 0.073 mm^2 by controls, respectively), whereas medial, adventitial, and whole vessel areas were not significantly influenced by RvD2 or MaR1 treatment at 14 days. Lumen area was not significantly increased by RvD2 and MaR1, although the smallest lumen group was the control-treated one. There were no differences in overall vessel size among the contralateral (noninjured) sides of the common carotid arteries from RvD2, MaR1, or vehicle treatment (data not shown).

DISCUSSION

The present report demonstrates that systemic administration of the DHA-derived proresolving lipid mediators RvD2 and MaR1 attenuates neointimal hyperplasia and vessel remodeling in a mouse model of arterial injury. We demonstrate reduced neutrophil and monocyte/macrophage recruitment, as well as increased M2 polarization in the arteries of treated mice. Early proliferation in the vessel wall was significantly reduced. Our *in vitro* studies suggest that these SPMs have direct effects on VSMCs including reduced migration to PDGF and altered response to inflammatory stimuli (TNF-α). Taken together these findings suggest that the mechanisms by which SPMs influenced neointima development in this model are likely related to alterations in both leukocyte–vessel wall interactions, as well as direct effects on the VSMC phenotype.

Bioactive lipid mediators such as prostaglandins, leukotrienes, and sphingolipids are known to play critical roles in the acute vascular responses to tissue injury and inflammation. Recent identification of a "resolution metabolome" based on the identification of SPMs derived from n-6 (arachidonic acid) and n-3 (EPA, DHA) fatty acids has expanded the biochemical understanding of homeostasis (6). These SPMs were initially isolated from inflammatory exudates in models of self-limited inflammation (19, 20). In recent advances, diseases based on protracted inflammation have been considered as potential therapeutic applications for the anti-inflammatory and "proresolving" effects of SPMs (5, 6). In prior studies, we provided evidence that SPM pathways and receptors are identified in injured vessels and directly mediate phenotypic changes in vascular cells (12, 13). The present work extends these observations to demonstrate the relevance of systemic augmentation of SPM pathways in the setting of acute flow-mediated vascular remodeling. The systemic dose protocol used here was empirical, based on a previous report in a mouse model of sepsis (20). These data collectively support the hypothesis that exaggerated neointimal hyperplasia may be linked to deficient resolution of the acute

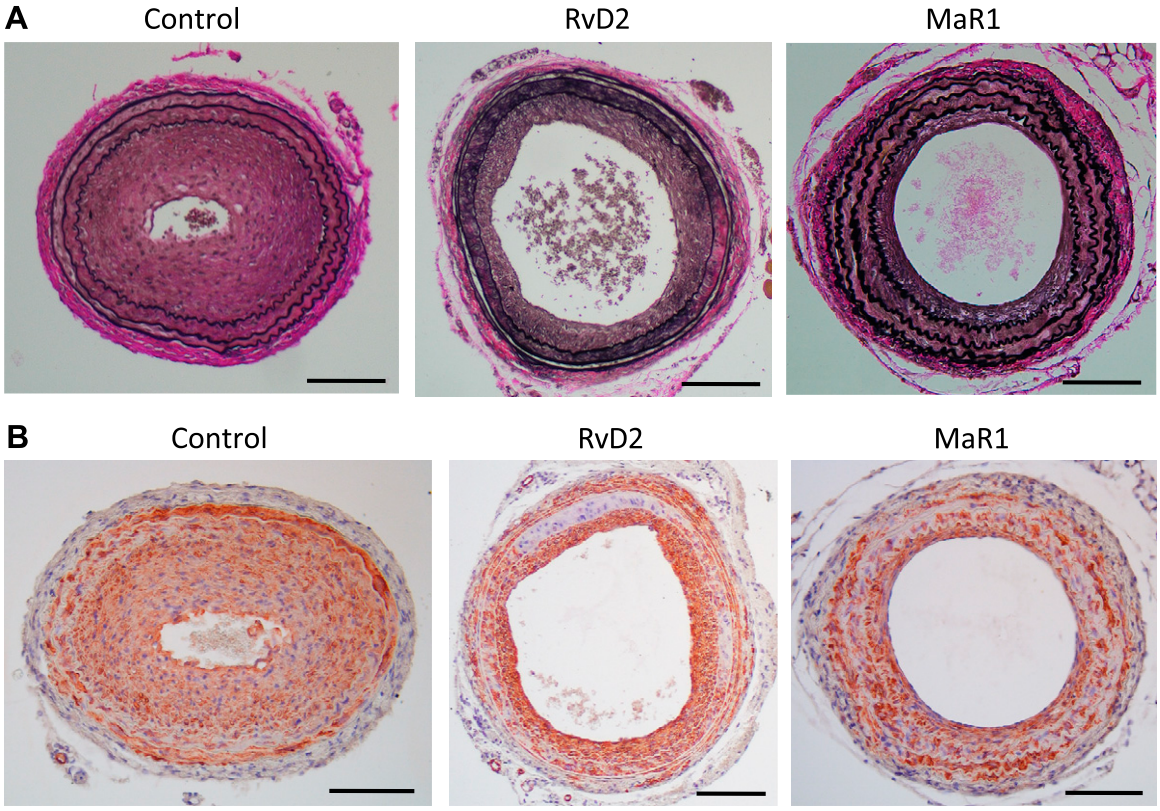

Figure 5. Vessel remodeling in the ligated carotid artery was modulated by systemic RvD2 and MaR1 treatment at 14 days. Controls were ligated arteries treated with vehicle. *A*) Representative photomicrographs of elastin staining are shown (bar, 100 μm). *B*) Representative photomicrographs of immunostaining of α-smooth muscle cell actin are shown (bar, 100 μm). Smooth muscle cells were mainly observed in neointima in all of 3 groups.

inflammatory response, generalizable across a broad spectrum of vascular injury and remodeling scenarios.

The characterization of the molecular circuits of resolution, including regulation of the synthetic pathways, identification of specific receptors in target cells, and downstream signaling events remain under active investigation. RvD2 was originally identified in resolving murine exudates and has shown biologic effects in murine models of peritonitis with sepsis (20), colitis (21), pain (22, 23), burns (24, 25), bone remodeling (26, 27), and metabolic syndrome (28). Specific receptors for RvD2 are not as yet identified; however, multiple lines of evidence including data presented here suggest that, like other SPMs, these are likely to include members of the G-protein coupled receptor family. MaR1 is a macrophage product also first identified in resolving mouse peritonitis exudates and demonstrating protective effects in models of colitis, lung injury, tissue regeneration, and inflammatory pain (8–10). Receptors for MaR1 are also unknown at the present time. Elucidation of these SPM receptors will be key to furthering the understanding of their mechanisms of action and subsequent therapeutic targeting.

In previous reports of carotid artery ligation in mice, low and oscillatory shear stress was observed, inflammatory genes were expressed, and reactive oxygen species production increased (29–31). Ligation of the carotid artery induces neointimal hyperplasia as a downstream outcome of vessel remodeling. Although different from an acute mechanical injury (*e.g.,* balloon or wire) and not performed in a background of atherosclerosis, the model has utility for examining the role of inflammation in the arterial injury response. Confirming other reports, we demonstrate that the neointima formed in this model over the first several weeks is comprised primarily of VSMCs. Migration and proliferation of VSMCs occur as a downstream result of increased growth factor and inflammatory mediator availability (17, 32, 33). Other reports have demonstrated reduced neointimal hyperplasia in this model by targeting inflammation (34, 35). Our results indicate that RvD2 and MaR1 administration was associated with significant effects on neointima formation in this model, without changes in overall vessel size. Given the overlapping effects of SPMs on resident vascular cell activity as well as leukocyte phenotype, we are unable to pinpoint a single specific mechanism as the primary driver of the altered arterial remodeling observed.

In the process of resolution of inflammation, the principal local leukocyte population converts from neutrophils to macrophages and the dominant macrophage phenotype switches from proinflammatory M1 to proresolving M2 (6). In our previous study of balloon angioplasty in rabbits, total leukocyte infiltration was reduced by local delivery of RvD2 (13). In the present study, we further characterize the acute effects of SPM on leukocyte recruitment and phenotype in arterial injury. RvD2 and MaR1 treatment decreased infiltration of polymorphonuclear leukocytes and monocytes/macrophages and altered the dominant macrophage phenotype toward M2.

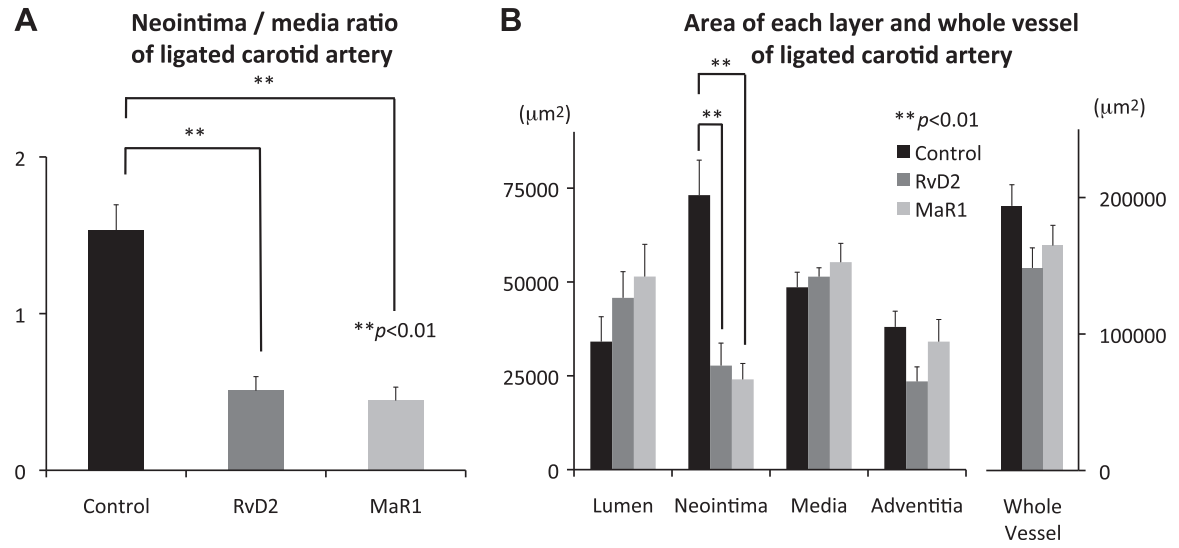

Figure 6. Systemic RvD2 and MaR1 treatment attenuates low flow-induced neointima formation in the mouse carotid artery at 14 days. Controls were ligated arteries treated with vehicle. *A*) Neointima/media ratio was significantly reduced by treatment by RvD2 (67%) or MaR1 (71%). *B*) Summary of morphometrical analysis shown as areas of each layer of injured arteries. Neointimal formation was attenuated by RvD2 (62%) or MaR1 (67%) treatment, although the areas of media, adventitia, lumen, and whole vessel were not changed by treatments. Values were measured as average of 3 sections for 1 artery ($n = 10$). $^{**}P < 0.01$ *vs.* control; Dunnett *post hoc* test. Results are means ± SE.

MCP-1 recruits monocytes to the sites of inflammation produced by either tissue injury or infection (36, 37). MCP-1 contributes to progression of atherosclerosis and acute myocardial infarction (38). We show that RvD2 and MaR1 suppressed MCP-1 expression from activated ASMCs. M2 macrophages play important roles for maintaining homeostasis against inflammation (39, 40) and atherosclerosis (41, 42). Resolvins stimulate conversion from M1 to M2 macrophages in several models (43, 44). Recent reports showed that a precursor of MaR1 shifted phenotype of macrophages from M1 to M2 *in vitro* (45). Phenotype switch from M1 to M2 induced by MaR1 was observed in an experimental colitis model *in vivo* (9). There are no prior reports of SPM effects on macrophage polarization in vascular injury. We speculate that the reduction in neutrophil recruitment and alteration in macrophage polarization are important for resolving inflammation and reducing neointima formation after vascular injury.

DHA is the precursor of both RvD2 and MaR1 and is largely derived in the human diet from marine sources. Intake of fish oil is considered as potentially protective against cardiovascular disease, although the existing evidence from clinical trials remains mixed. It is currently unknown whether supplementation of n-3 PUFAs could reduce neointimal hyperplasia after vascular intervention or surgery. It is noteworthy that recent studies suggest that short-term high-dose nutritional supplementation with fish oil can alter the lipid metabolome in subjects with peripheral artery disease, suggesting the basis for further interventional trials in this population (46). In summary, our study demonstrates that systemic administration of 2 DHA-derived SPMs (RvD2 and MaR1) attenuates low flow-induced arterial remodeling in mice, likely *via* effects on leukocyte trafficking, macrophage, and VSMC phenotype. Augmentation of resolution by local or systemic delivery of the bioactive SPM, or their biochemical precursors, may have beneficial effects on vascular healing. FJ

The authors thank Dr. Giorgio Mottola, who provided technical and analytic support for the scratch migration assays. This work was supported in part by the U.S. National Institutes of Health, National Heart, Lung, and Blood Institute Grant HL119508 (to M.S.C.).

REFERENCES

1. Fowkes, F. G., Rudan, D., Rudan, I., Aboyans, V., Denenberg, J. O., McDermott, M. M., Norman, P. E., Sampson, U. K., Williams, L. J., Mensah, G. A., and Criqui, M. H. (2013) Comparison of global estimates of prevalence and risk factors for peripheral artery disease in 2000 and 2010: a systematic review and analysis. *Lancet* **382**, 1329–1340
2. Saw, J., Bhatt, D. L., Moliterno, D. J., Brener, S. J., Steinhubl, S. R., Lincoff, A. M., Tcheng, J. E., Harrington, R. A., Simoons, M., Hu, T., Sheikh, M. A., Kereiakes, D. J., and Topol, E. J. (2006) The influence of peripheral arterial disease on outcomes: a pooled analysis of mortality in eight large randomized percutaneous coronary intervention trials. *J. Am. Coll. Cardiol.* **48**, 1567–1572
3. Jones, D. W., Schanzer, A., Zhao, Y., MacKenzie, T. A., Nolan, B. W., Conte, M. S., and Goodney, P. P.; Vascular Study Group of New England. (2013) Growing impact of restenosis on the surgical treatment of peripheral arterial disease. *J Am Heart Assoc* **2**, e000345
4. Ross, R. (1999) Atherosclerosis—an inflammatory disease. *N. Engl. J. Med.* **340**, 115–126
5. Fredman, G., and Serhan, C. N. (2011) Specialized proresolving mediator targets for RvE1 and RvD1 in peripheral blood and mechanisms of resolution. *Biochem. J.* **437**, 185–197
6. Serhan, C. N. (2014) Pro-resolving lipid mediators are leads for resolution physiology. *Nature* **510**, 92–101
7. Serhan, C. N., Yang, R., Martinod, K., Kasuga, K., Pillai, P. S., Porter, T. F., Oh, S. F., and Spite, M. (2009) Maresins: novel macrophage mediators with potent antiinflammatory and proresolving actions. *J. Exp. Med.* **206**, 15–23
8. Gong, J., Wu, Z. Y., Qi, H., Chen, L., Li, H. B., Li, B., Yao, C. Y., Wang, Y. X., Wu, J., Yuan, S. Y., Yao, S. L., and Shang, Y. (2014) Maresin 1 mitigates lipopolysaccharide-induced acute lung injury in mice. *Br. J. Pharmacol.* **171**, 3539–3550
9. Marcon, R., Bento, A. F., Dutra, R. C., Bicca, M. A., Leite, D. F., and Calixto, J. B. (2013) Maresin 1, a proresolving lipid mediator derived from omega-3 polyunsaturated fatty acids, exerts protective actions in murine models of colitis. *J. Immunol.* **191**, 4288–4298

10. Serhan, C. N., Dalli, J., Karamnov, S., Choi, A., Park, C. K., Xu, Z. Z., Ji, R. R., Zhu, M., and Petasis, N. A. (2012) Macrophage proresolving mediator maresin 1 stimulates tissue regeneration and controls pain. *FASEB J.* **26**, 1755–1765
11. Merched, A. J., Ko, K., Gotlinger, K. H., Serhan, C. N., and Chan, L. (2008) Atherosclerosis: evidence for impairment of resolution of vascular inflammation governed by specific lipid mediators. *FASEB J.* **22**, 3595–3606
12. Ho, K. J., Spite, M., Owens, C. D., Lancero, H., Kroemer, A. H., Pande, R., Creager, M. A., Serhan, C. N., and Conte, M. S. (2010) Aspirin-triggered lipoxin and resolvin E1 modulate vascular smooth muscle phenotype and correlate with peripheral atherosclerosis. *Am. J. Pathol.* **177**, 2116–2123
13. Miyahara, T., Runge, S., Chatterjee, A., Chen, M., Mottola, G., Fitzgerald, J. M., Serhan, C. N., and Conte, M. S. (2013) D-series resolvin attenuates vascular smooth muscle cell activation and neointimal hyperplasia following vascular injury. *FASEB J.* **27**, 2220–2232
14. Geisterfer, A. A., Peach, M. J., and Owens, G. K. (1988) Angiotensin II induces hypertrophy, not hyperplasia, of cultured rat aortic smooth muscle cells. *Circ. Res.* **62**, 749–756
15. Ho, K. J., Owens, C. D., Longo, T., Sui, X. X., Ifantides, C., and Conte, M. S. (2008) C-reactive protein and vein graft disease: evidence for a direct effect on smooth muscle cell phenotype *via* modulation of PDGF receptor-beta. *Am. J. Physiol. Heart Circ. Physiol.* **295**, H1132–H1140
16. Li, P., Zhu, N., Yi, B., Wang, N., Chen, M., You, X., Zhao, X., Solomides, C. C., Qin, Y., and Sun, J. (2013) MicroRNA-663 regulates human vascular smooth muscle cell phenotypic switch and vascular neointimal formation. *Circ. Res.* **113**, 1117–1127
17. Kumar, A., and Lindner, V. (1997) Remodeling with neointima formation in the mouse carotid artery after cessation of blood flow. *Arterioscler. Thromb. Vasc. Biol.* **17**, 2238–2244
18. Serhan, C. N., Clish, C. B., Brannon, J., Colgan, S. P., Chiang, N., and Gronert, K. (2000) Novel functional sets of lipid-derived mediators with antiinflammatory actions generated from omega-3 fatty acids *via* cyclooxygenase 2-nonsteroidal antiinflammatory drugs and transcellular processing. *J. Exp. Med.* **192**, 1197–1204
19. Serhan, C. N., Hong, S., Gronert, K., Colgan, S. P., Devchand, P. R., Mirick, G., and Moussignac, R. L. (2002) Resolvins: a family of bioactive products of omega-3 fatty acid transformation circuits initiated by aspirin treatment that counter proinflammation signals. *J. Exp. Med.* **196**, 1025–1037
20. Spite, M., Norling, L. V., Summers, L., Yang, R., Cooper, D., Petasis, N. A., Flower, R. J., Perretti, M., and Serhan, C. N. (2009) Resolvin D2 is a potent regulator of leukocytes and controls microbial sepsis. *Nature* **461**, 1287–1291
21. Bento, A. F., Claudino, R. F., Dutra, R. C., Marcon, R., and Calixto, J. B. (2011) Omega-3 fatty acid-derived mediators 17(R)-hydroxy docosahexaenoic acid, aspirin-triggered resolvin D1 and resolvin D2 prevent experimental colitis in mice. *J. Immunol.* **187**, 1957–1969
22. Park, C. K., Xu, Z. Z., Liu, T., Lü, N., Serhan, C. N., and Ji, R. R. (2011) Resolvin D2 is a potent endogenous inhibitor for transient receptor potential subtype V1/A1, inflammatory pain, and spinal cord synaptic plasticity in mice: distinct roles of resolvin D1, D2, and E1. *J. Neurosci.* **31**, 18433–18438
23. Klein, C. P., Sperotto, N. D., Maciel, I. S., Leite, C. E., Souza, A. H., and Campos, M. M. (2014) Effects of D-series resolvins on behavioral and neurochemical changes in a fibromyalgia-like model in mice. *Neuropharmacology* **86**, 57–66
24. Bohr, S., Patel, S. J., Sarin, D., Irimia, D., Yarmush, M. L., and Berthiaume, F. (2013) Resolvin D2 prevents secondary thrombosis and necrosis in a mouse burn wound model. *Wound Repair Regen.* **21**, 35–43
25. Kurihara, T., Jones, C. N., Yu, Y. M., Fischman, A. J., Watada, S., Tompkins, R. G., Fagan, S. P., and Irimia, D. (2013) Resolvin D2 restores neutrophil directionality and improves survival after burns. *FASEB J.* **27**, 2270–2281
26. Steffens, J. P., Herrera, B. S., Coimbra, L. S., Stephens, D. N., Rossa, C., Jr., Spolidorio, L. C., Kantarci, A., and Van Dyke, T. E. (2014) Testosterone regulates bone response to inflammation. *Horm. Metab. Res.* **46**, 193–200
27. McCauley, L. K., Dalli, J., Koh, A. J., Chiang, N., and Serhan, C. N. (2014) Cutting edge: Parathyroid hormone facilitates macrophage efferocytosis in bone marrow *via* proresolving mediators resolvin D1 and resolvin D2. *J. Immunol.* **193**, 26–29
28. Katakura, M., Hashimoto, M., Inoue, T., Al Mamun, A., Tanabe, Y., Iwamoto, R., Arita, M., Tsuchikura, S., and Shido, O. (2014) Omega-3 fatty acids protect renal functions by increasing docosahexaenoic acid-derived metabolite levels in SHR.Cg-Lepr(cp)/NDmcr rats, a metabolic syndrome model. *Molecules* **19**, 3247–3263
29. Godin, D., Ivan, E., Johnson, C., Magid, R., and Galis, Z. S. (2000) Remodeling of carotid artery is associated with increased expression of matrix metalloproteinases in mouse blood flow cessation model. *Circulation* **102**, 2861–2866
30. Khatri, J. J., Johnson, C., Magid, R., Lessner, S. M., Laude, K. M., Dikalov, S. I., Harrison, D. G., Sung, H. J., Rong, Y., and Galis, Z. S. (2004) Vascular oxidant stress enhances progression and angiogenesis of experimental atheroma. *Circulation* **109**, 520–525
31. Nam, D., Ni, C. W., Rezvan, A., Suo, J., Budzyn, K., Llanos, A., Harrison, D., Giddens, D., and Jo, H. (2009) Partial carotid ligation is a model of acutely induced disturbed flow, leading to rapid endothelial dysfunction and atherosclerosis. *Am. J. Physiol. Heart Circ. Physiol.* **297**, H1535–H1543
32. Kumar, A., Hoover, J. L., Simmons, C. A., Lindner, V., and Shebuski, R. J. (1997) Remodeling and neointimal formation in the carotid artery of normal and P-selectin-deficient mice. *Circulation* **96**, 4333–4342
33. Holt, A. W., and Tulis, D. A. (2013) Experimental Rat and Mouse Carotid Artery Surgery: Injury & Remodeling Studies. *ISRN Minim Invasive Surg* **2013**, 167407
34. Petri, M. H., Laguna-Fernandez, A., Tseng, C. N., Hedin, U., Perretti, M., and Bäck, M. (2015) Aspirin-triggered 15-epi-lipoxin A_4 signals through FPR2/ALX in vascular smooth muscle cells and protects against intimal hyperplasia after carotid ligation. *Int. J. Cardiol.* **179**, 370–372
35. Korshunov, V. A., Nikonenko, T. A., Tkachuk, V. A., Brooks, A., and Berk, B. C. (2006) Interleukin-18 and macrophage migration inhibitory factor are associated with increased carotid intima-media thickening. *Arterioscler. Thromb. Vasc. Biol.* **26**, 295–300
36. Carr, M. W., Roth, S. J., Luther, E., Rose, S. S., and Springer, T. A. (1994) Monocyte chemoattractant protein 1 acts as a T-lymphocyte chemoattractant. *Proc. Natl. Acad. Sci. USA* **91**, 3652–3656
37. Xu, L. L., Warren, M. K., Rose, W. L., Gong, W., and Wang, J. M. (1996) Human recombinant monocyte chemotactic protein and other C-C chemokines bind and induce directional migration of dendritic cells in vitro. *J. Leukoc. Biol.* **60**, 365–371
38. Xia, M., and Sui, Z. (2009) Recent developments in CCR2 antagonists. *Expert Opin Ther Pat* **19**, 295–303
39. Fujiu, K., Wang, J., and Nagai, R. (2014) Cardioprotective function of cardiac macrophages. *Cardiovasc. Res.* **102**, 232–239
40. Wynn, T. A., Chawla, A., and Pollard, J. W. (2013) Macrophage biology in development, homeostasis and disease. *Nature* **496**, 445–455
41. Danenberg, H. D., Fishbein, I., Gao, J., Mönkkönen, J., Reich, R., Gati, I., Moerman, E., and Golomb, G. (2002) Macrophage depletion by clodronate-containing liposomes reduces neointimal formation after balloon injury in rats and rabbits. *Circulation* **106**, 599–605
42. Stoneman, V., Braganza, D., Figg, N., Mercer, J., Lang, R., Goddard, M., and Bennett, M. (2007) Monocyte/macrophage suppression in CD11b diphtheria toxin receptor transgenic mice differentially affects atherogenesis and established plaques. *Circ. Res.* **100**, 884–893
43. Titos, E., Rius, B., González-Périz, A., López-Vicario, C., Morán-Salvador, E., Martínez-Clemente, M., Arroyo, V., and Clària, J. (2011) Resolvin D1 and its precursor docosahexaenoic acid promote resolution of adipose tissue inflammation by eliciting macrophage polarization toward an M2-like phenotype. *J. Immunol.* **187**, 5408–5418
44. Hsiao, H. M., Sapinoro, R. E., Thatcher, T. H., Croasdell, A., Levy, E. P., Fulton, R. A., Olsen, K. C., Pollock, S. J., Serhan, C. N., Phipps, R. P., and Sime, P. J. (2013) A novel anti-inflammatory and pro-resolving role for resolvin D1 in acute cigarette smoke-induced lung inflammation. *PLoS ONE* **8**, e58258
45. Dalli, J., Zhu, M., Vlasenko, N. A., Deng, B., Haeggström, J. Z., Petasis, N. A., and Serhan, C. N. (2013) The novel 13S,14S-epoxy-maresin is converted by human macrophages to maresin 1 (MaR1), inhibits leukotriene A4 hydrolase (LTA4H), and shifts macrophage phenotype. *FASEB J.* **27**, 2573–2583
46. Nosova, E. V., Chong, K. C., Alley, H. F., Harris, W. S., Boscardin, W. J., Conte, M. S., Owens, C. D., and Grenon, S. M. (2014) Clinical correlates of red blood cell omega-3 fatty acid content in male veterans with peripheral arterial disease. *J. Vasc. Surg.* **60**, 1325–1331

Received for publication October 3, 2014.
Accepted for publication February 9, 2015.